A control theoretic approach to evaluate and inform ecological momentary interventions

Janik Fechtelpeter[1*], Christian Rauschenberg[2], Hamidreza Jalalabadi[3], Benjamin Boecking[4], Therese van Amelsvoort[5], Ulrich Reininghaus[2,6,7], Daniel Durstewitz[1,8,9†], Georgia Koppe[1,10,11†]

[1]Dept. of Theoretical Neuroscience, Central Institute of Mental Health (CIMH), Medical Faculty Mannheim, Heidelberg University, Germany.
[2]Dept. of Public Mental Health, CIMH, Medical Faculty Mannheim, Heidelberg University, Germany.
[3]Dept. of Psychiatry and Psychotherapy, Philipps University of Marburg, Germany.
[4]Charité, University Hospital Berlin, Germany.
[5]Dept. of Psychiatry and Neuropsychology, School for Mental Health and Neuroscience, Maastricht University, Netherlands.
[6]Centre for Epidemiology and Public Health, Health Service and Population Research Dept., Institute of Psychiatry, Psychology & Neuroscience, King's College London, UK.
[7]ESRC Centre for Society and Mental Health, King's College London, UK.
[8]Faculty of Physics and Astronomy, Heidelberg University, Germany.
[9]Interdisciplinary Center for Scientific Computing, Heidelberg University, Germany.
[10]Dept. of Psychiatry and Psychotherapy, CIMH, Medical Faculty Mannheim, Heidelberg University, Germany.
[11]Hector Institute for Artificial Intelligence in Psychiatry, CIMH, Medical Faculty Mannheim, Heidelberg University, Germany.

*Corresponding author(s). E-mail(s): janik.fechtelpeter@zi-mannheim.de;
†These authors contributed equally to this work.

Abstract

Ecological momentary interventions (EMI) are digital mobile health (mHealth) interventions that are administered in an individual's daily life with the intent to improve mental health outcomes by tailoring intervention components to person, moment, and context. Questions regarding which intervention is most effective in a given individual, when it is best delivered, and what mechanisms of change underlie observed effects therefore naturally arise in this setting. To achieve this, EMI are typically informed by the collection of multivariate intensive longitudinal data of various target constructs - designed to assess an individual's psychological state - using ecological momentary assessments (EMA). However, the dynamic and interconnected nature of such multivariate time series data poses several challenges when analyzing and interpreting findings. This may be illustrated when understanding psychological variables as part of an interconnected network of dynamic variables, and the delivery of EMI as time-specific perturbations to these variables. Network control theory (NCT) is a branch of dynamical systems theory that precisely deals with the formal analysis of such network perturbations and provides solutions of how to perturb a network to reach a desired state in an optimal manner. In doing so, NCT may help to formally quantify and evaluate proximal intervention effects, as well as to identify optimal intervention approaches given a set of reasonable (temporal or energetic) constraints. In this proof-of-concept study, we leverage concepts from NCT to analyze the data of 10 individuals undergoing joint EMA and EMI for several weeks. We show how simple metrics derived from NCT can provide insightful information on putative mechanisms of change in the inferred EMA networks and contribute to identifying optimal leveraging points. We also outline what additional considerations might play a role in the design of effective intervention strategies in the future from the perspective of NCT.

Keywords: ecological momentary assessment, ecological momentary intervention, mental health, mobile health, digital intervention, control theory, linear dynamical systems, computational psychiatry

1 Introduction

Mobile devices such as smartphones and sensors allow us to collect rich and dynamic information about an individual's mental state (e.g.,[1–4]). For example, ecological momentary assessments (EMA) enable to collect high-dimensional information on positive and negative affect, physical needs, and social interaction several times a day [5], sometimes over periods of months [6]. A central advantage of these approaches is that mental health states are sampled within the everyday life and context of an individual. Through these *ecologically valid* assessments, we can obtain more detailed insight into the actual time points at which mental health declines. This paves the way to explore and identify immediately preceding or succeeding maladaptive behavioral patterns, and to intervene at critical time points. It has been argued that interventions delivered at these moments may therefore be most profitable [5, 7].

Ecological momentary interventions (EMI) represent a specific type of mobile health (mHealth) interventions that aim to fill this critical gap in the treatment of mental health conditions. EMI are administered via smartphone devices and are designed to intervene in an individual's natural environment, precisely at moments when mental health is at risk [7–9]. For instance, the administration of EMI has been used to improve resilience in response to stress in youth at risk to develop, or with first episodes of severe mental disorders [2, 10, 11], and to reduce depression and anxiety [**? ?**]. EMI may also be particularly effective in mental health promotion as well as preventing poor mental health outcomes in youth, given their generally positive attitude towards mHealth applications [10]. Moreover, for service users which frequently experience psychiatric symptoms that may be triggered by the exposure to socio-environmental risk factors, EMI provide a window of opportunity for supplementing traditional face-to-face therapy (i.e., blended care) [13, 14].

While the combination of EMA and EMI bears great potential for alleviating mental health burden, it also poses several data analytic challenges. For instance, when using EMA to evaluate the (proximal) success of an intervention delivery, we need to account for the temporal dynamics and the interdependencies of the sampled EMA variables (e.g., [12, 15, 16]). Through interdependencies and feedback mechanisms between different psychological variables, it is conceivable for instance, that seemingly small immediate effects accumulate to large effects over time, or alternatively, that an intervention may have an immediate favorable effect on the mental state, but backfires with time (see also [15, 17, 18]). When evaluating proximal intervention effects, we may want to account for all of these (possibly counterintuitive) patterns, as well as obtain a clear picture on its mechanisms of change. However, isolating intervention effects in time-varying EMA and tracking them over time can become challenging (particularly for high-dimensional recordings). Also, when personalizing an intervention – that is, when seeking to identify and present the most effective intervention for a specific individual at a given time – we may need to factor in inter-individual differences in these dynamics (see also [19, 20]). Finally, different researchers may want to improve different outcomes (e.g., some may want to reduce negative affect while others aim to increase activity levels [18]). Yet, an overarching framework to deliver personalized EMI would be favorable.

One way to address these challenges is to understand and treat the psychological variables collected within an EMA as an interconnected dynamic network [15, 17, 21–25]. By operating on such networks, network control theory (NCT) offers guidelines and insights on how to address current questions in EMI research [17]. NCT is a contemporary branch of dynamical systems theory which concerns itself with quantifying the control an external input (such as an intervention) exerts over a dynamical system (DS) such as a network of psychological or mental health variables. Specifically, NCT studies how a network behaves under perturbation both immediately and over time, and how to place perturbations to achieve some goal or desired state [26]. In this way, NCT provides insight into which individuals are particularly sensitive to interventions based on their network structure, and which nodes (e.g., which EMA variables) are best to target in order to effect change. The latter is particularly relevant when it comes to designing and refining user-friendly and personalized EMI delivery schemes,

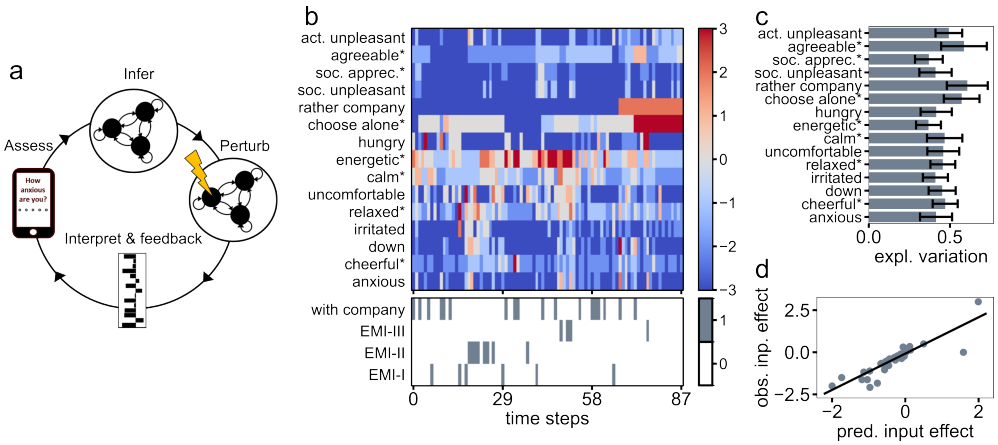

Fig. 1 Proposed framework and goodness of fit. (A) Proposed analysis approach. After assessing EMA and EMI time series, we infer dynamical systems models on these time series and conduct perturbation analyses to obtain insights into network control and future system behavior. (B) Example of EMA time series of one participant (top) and presented inputs (bottom). (C) Average explained variation (x-axis) in EMA variables (y-axis) by inferred LDS models (mean and SEM are displayed). (D) Observed (y-axis) vs. predicted (x-axis) immediate input effects averaged over participants.

or when aiming to gain insights into an individual's behavioral contingencies, that may, in turn, be addressed in conventional psychotherapy.

In a proof-of-concept study, we aimed to illustrate these principles on a dataset of individuals that underwent several weeks of EMI for the improvement of emotional resilience in youth with early mental health problems (i.e., EMIcompass) [10]. We used NCT to identify network nodes which have high impact and high reach on mental health states, to evaluate effects of real and hypothetical interventions over time, and to outline the considerations necessary to address the ambitious goal of designing an optimal EMI delivery scheme.

2 Results

Ten participants underwent several weeks of EMA with interleaved EMI. Table 1 lists the assessed EMA variables while Figure 1a illustrates our approach. To extract the dynamics and the associated network structure underlying these time series (see Figure 1a for an example), we modeled the EMA time series as a linear dynamical system (LDS; cf. Methods "Dynamical system models"), where the EMI constitute external inputs, that is, perturbations, to this system. The dynamics and network structure of each participant are described by the following map:

$$x_{t+1} = Ax_t + Bu_t.$$

Here, x_t is a (state) vector collecting all EMA scores at time t, A is an adjacency matrix which describes how different vector elements (linearly) affect each other from one time point to the next (that is, A describes the network structure), u_t are vectors

coding for the presence of different external inputs at time t, and B is a matrix specifying the degree to which each external input perturbs the system state. The external inputs consist of binary vectors which indicate the delivery of three types of EMI (with a 1 indicating a delivery), or whether the individual was currently alone or in the presence of social company (a 1 indicating company; see also Methods "EMI and input data"). Using NCT, we examined i) the networks' responses to EMI as well as simulated interventions on single nodes in detail, and ii) the optimal control policies and their implications for EMA and EMI research.

2.1 Goodness of fit

Before analyzing network control in detail, we first assessed how well the inferred LDS models captured the dynamics in the observed data. Figure 1c depicts the explained variation in each EMA variable averaged over all participants. On average, the fraction of variance explained by the LDS models in the observer time series was $R^2 = .46$ (standard deviation .28). Immediate intervention effects, that is, differences in EMA scores immediately before and after presentation of an input averaged across participants, were predicted with $R^2 = 0.78$ ($p < .001$; see Figure 1d).

2.2 Controllability

Having established that the LDS models account for a significant proportion of variance in the original time series and were successful at predicting relative input effects, we next tested whether the inferred systems are controllable through the presented inputs and through hypothetical interventions on single network nodes (i.e., through perturbing single EMA variables). We use the term intervention here to refer to a control matrix and unit input acting on the network (cf. Methods). Controllability is assessed by evaluating the rank of the controllability Gramian (eqn. (2)) and means that a given network is structured such that the administered intervention may in principle drive it into any desired outcome state (assuming that we can select an arbitrary control input sequence). Most but not all networks were controllable by the each presented EMI individually (Figure 2a). The two participants that were not controllable by any of the EMI, were yet controllable by interventions designed to target specific network nodes. This suggests that one could in principle design an intervention by which to control these individuals as well.

2.3 Average controllability

Controllability may provide important insights into an individual's general network structure by indicating which state configurations are per se unreachable through intervention. In practice however, it may be difficult to deploy interventions to control systems to such a degree as to steer the network into any desired state (even if they are controllable). This relates to the fact that we cannot arbitrarily scale EMI effects (in contrast, for instance, to an electronic circuit where an input current can be increased by orders of magnitude). Of greater practical relevance is therefore the question to what degree a system is controllable by a given intervention, and accordingly, whether we can identify specific EMI or network nodes that facilitate system control. Such

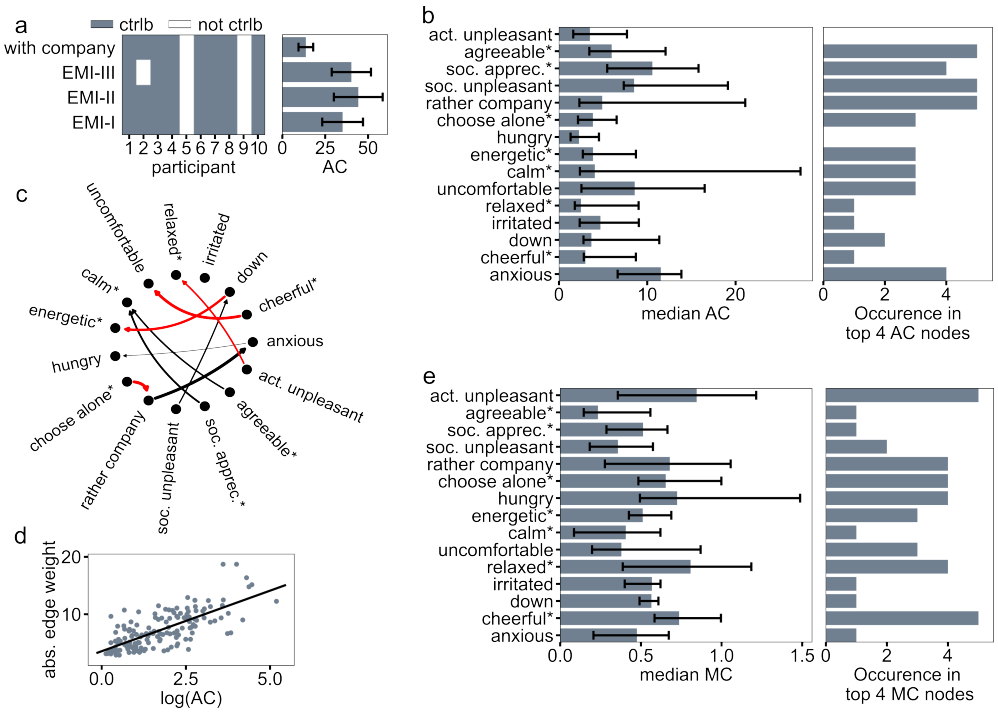

Fig. 2 Controllability metrics. (A) Left: System controllability of each participant (x-axis) by presented external inputs (y-axis). Most but not all systems were controllable (ctrlb) by the presented inputs. Right: Average controllability (AC) of presented inputs (mean and SEM are displayed). (B) Left: AC of single network nodes (median and 25-75 percentile range are displayed). Right: Distribution over the number of times each node was identified as one of the top 4 highest AC nodes in each individual. (C) Adjacency A matrix averaged across participants and thresholded for connections significant at $p < .05$ (uncorrected for multiple testing) as identified via t-tests for visualization purposes (arrow width indicates average strength, positive/negative connections in black/red). (D) Correlation between log AC per node (x-axis) and sum over absolute incoming and outcoming edge weights of each node. (E) Left: Modal controllability (MC) of single network nodes (mean and SEM are displayed). Right: Distribution over the number of times each node was identified as one of the top 4 highest MC nodes in each individual.

analyses can deliver insights into working mechanisms of a network and may provide efficient strategies for future treatment. Average controllability (AC) quantifies the degree of control exerted by an intervention (cf. Methods "Average controllability"). Loosely speaking, it quantifies the ability of an intervention to cause large state changes with little input energy, steering the system into easy-to-reach states (e.g., [27–29]).

As interventions, we evaluated the three delivered EMI and an external input indicating the presence or absence of social company. The right hand side of Figure 2a displays the mean AC of each intervention. Overall, we found an indication that the designed EMI exerted stronger control over the inferred systems than the mere presence or absence of social company ($T(9) = 2.056$, $p = 0.07$, Figure 2a). We did, however, observe a large variation in AC across individuals (with standard deviations

[SD] ranging between 12.8 and 42.7 for the four inputs, respectively). This suggests that the degree of control exerted by each input strongly depends on inter-individual differences in dynamics.

We also evaluated simulated (hypothetical) interventions that we designed to target single network nodes separately. These observations are consistent with results obtained from EMI and presence of company (see Figure 2b). Node-wise AC showed high variations across participants (see Figure 2b for percentile ranges). This variation coincided with a high degree of inter-individual differences in network structure. Network edge weights exhibited high variance, and no consistent pattern for positive or negative weights across individuals could be confirmed by t-tests (all $p_{\text{Bonf}} > .05$; although multiple test corrections may have limited these findings in light of the small sample; see Figure 2c for uncorrected exploratory results). Collectively, these findings signal substantial inter-individual differences in system responses, which may demand and further support the importance of personalized (rather than group-based) intervention strategies (see also [19, 20]).

Nonetheless, we also found evidence for a few common nodes with high AC across individuals. For instance, 'social unpleasantness', 'agreeable*', and 'rather company' (reflecting an individual's desire to rather be with company when alone) were frequently identified among the four nodes with highest AC in each individual (identified in 5 out of 10 individuals, Figure 2b right). Moreover, 'anxious' was the node with highest median AC (Figure 2b left), also exerting a high degree of average control over the inferred DS.

Nodes which exert high average control are typically hub nodes [27], i.e., nodes with strong connections to (often multiple) other nodes. This could be confirmed here as well, with log AC being positively associated with the log net magnitude of incoming and outgoing edge weights of a given node (see Figure 2d; $r = .71,\ p < .001$). The results implicate that interventions that particularly target social-cognitive processes, or anxiety, can be expected to have a strong impact on the system state across individuals.

2.4 Modal controllability

In contrast to AC, which quantifies control via easy-to-reach states, modal controllability (MC) identifies nodes that can steer the system into difficult directions. MC refers to the ability of a node to change the system state along all of its modes (that is, a set of linearly independent directions in state space; cf. Methods "Modal controllability"), independent of input (see eqn. (3)). Here, we identify feeling 'hungry', 'activity unpleasantness', and feeling 'relaxed*' as those with descriptively highest median MC (Figure 2e). 'Cheerfulness*' and 'activity unpleasantness' were identified among the 4 nodes with highest MC (identified in 5 out of 10 individuals). Log MC scores were negatively correlated with log AC ($r = -.76,\ p < .001$), and only slightly negatively correlated with edge weight magnitude ($r = -.26, p = .001$), consistent with previous observations of high MC nodes not being network hubs [27].

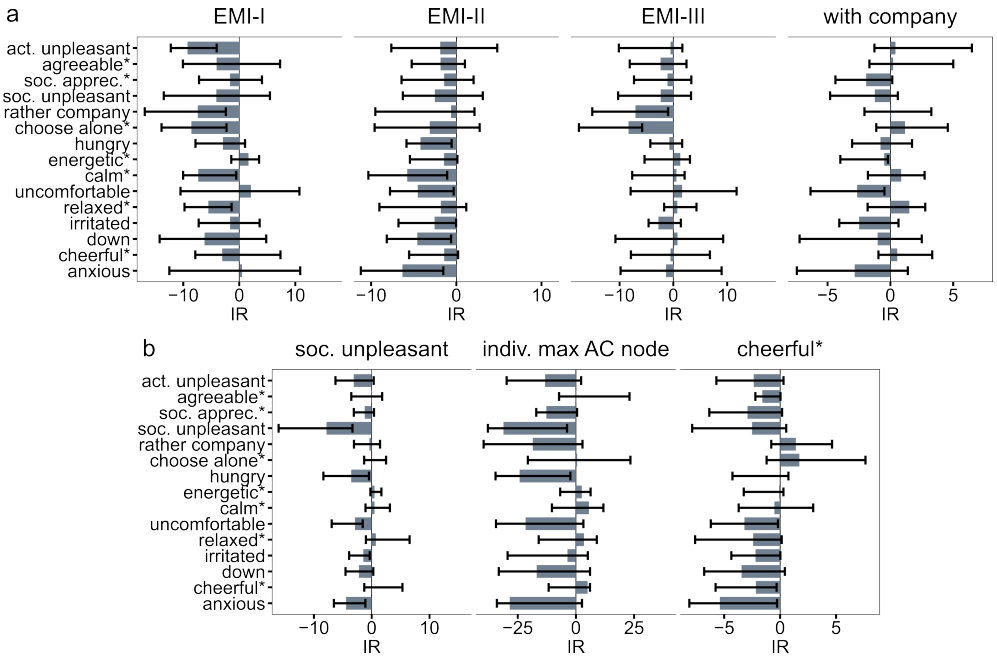

Fig. 3 Cumulative impulse response. (A) Predicted network cumulative impulse response (CIR) for 100 time steps in response to the four presented inputs (median and 25-75 percentile range are displayed). Negative values always indicate an improvement in observed variables since an unfavorable mental health state is reduced. Asterisks mark inverted scales. (B) Left: Same as (A) for network node frequently identified as having high AC across participants. Middle: Same as left side, for the maximum AC node for each individual. Right: Same as left side for network node with frequently high MC.

2.5 Cumulative impulse response

2.5.1 Presented inputs

While AC and MC are directly related and interpretable in terms of the systems' eigenvector basis, many times we may be more interested in quantifying the predicted proximal or distal effect of an intervention in the observable space, that is, in terms of the assessed EMA. Since these effects depend on the interconnections of all nodes, they are difficult to disentangle by a mere inspection of time series values. Here, we quantify these effects by looking at the network's cumulative impulse response (CIR) to an input, that is, the cumulative effect an input exerts on the system state over time considering all network connections (cf. Methods "Cumulative impulse response"; eqn. (4)). We ask 'what is the expected proximal effect of a given intervention on each psychological variable over time'?

Figure 3a shows the predicted median CIR integrated over 100 time steps for the three EMI and the social external input (indicating the presence or absence of social company). EMI-I and EMI-II resulted in an improvement across the assessed

psychological variables, predicted by a general decrease in predicted median CIR (EMI-I: $T(14) = -4.15,\ p_{\text{Bonf}} = .004$, EMI-II: $T(14) = -6.55,\ p_{\text{Bonf}} < .001$, EMI-III: $T(14) = -2.00,\ p_{\text{Bonf}} = .26$). Increasing the desire to be alone did not improve the mental state ($T(14) = -1.58,\ p_{\text{Bonf}} = .55$, p values were Bonferroni corrected for four tests.

2.5.2 Single network nodes

Whereas Figure 3a demonstrates how NCT may be applied to evaluate actual interventions, it may also be leveraged to simulate other interventions that were never actually presented. Here we simulated interventions targeting each single network node separately, by perturbing it into the negative direction (and thus, expecting a favorable mental health outcome). Figure 3b delineates the (100 time step) CIR for simulated interventions which target EMA nodes with a frequently high AC ('soc. unpleasantness'; figure 3b left), a frequently high MC ('cheerfulness*'; figure 3b right), and the node with highest AC in each individual participant (Figure 3b middle). Interventions on the identified high AC nodes statistically reduced the CIR scores ('social unpleasantness': $T(14) = -2.77,\ p_{\text{Bonf}} = .046$, personalized AC nodes: $T(14) = -3.07\ p_{\text{Bonf}} = .029$). Among these two interventions, the personalized intervention which targeted the highest AC node in each individual was superior in improving mental health than targeting 'social unpleasantness' ($T(14) = 3.04,\ p = .009$). The results are consistent with the notion that decreasing social unpleasantness results in a favorable mental health state, and that personalized interventions which target the highest AC node in each individual can be (even more) effective in improving mental health.

However, although predominantly reducing unhealthy states, the two high AC interventions also exerted an unfavorable effect on several variables (e.g., they tended to reduced feeling calm or cheerful). This was not the case when targeting 'cheerfulness*' (a node with frequently high MC). Targeting 'cheerfulness*' had a moderate but consistent and significant impact on improving the mental health state ($T(14) = -3.487,\ p_{\text{Bonf}} = .011$). Overall, intervention effects again varied quite largely across participants (see Figure 3b left and right), necessitating future replication and/or further evidence for personalized intervention strategies.

2.6 Optimal treatment policies

Eqn. (1) defines a dynamical system that - once inferred - determines the future fate of the network of EMA variables, and relatedly, the system's future response to proposed interventions. This property in principle allows us not only to evaluate the effect of administered and hypothetical interventions, but also to identify optimal treatment policies. An optimal treatment policy refers to a personalized sequence of proposed interventions that optimizes the predicted EMA variables in a user-defined sense. The goal is to drive the system into a desired state, where the type of state, the speed of convergence towards this state, as well as the amount of input energy needed to reach this state are user-defined. NCT provides a principled (and well-defined) approach towards identifying such optimal solutions (see eqn. (5)). In this section, we investigate such optimal control policies and relate them to AC and MC.

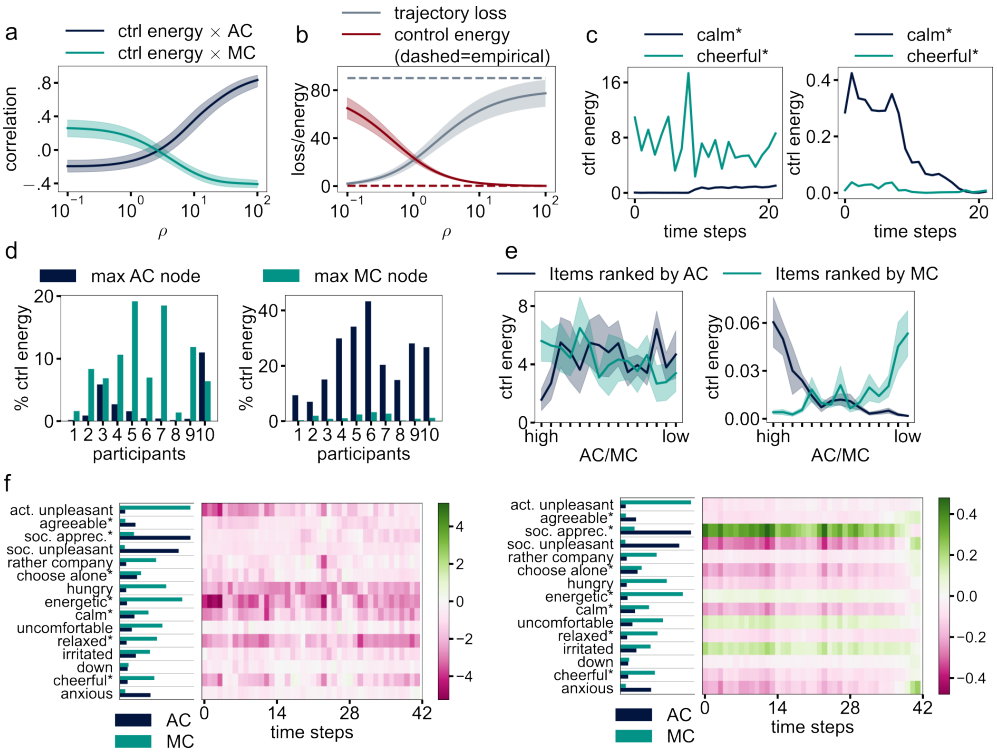

Fig. 4 Optimal treatment policies. (A) Correlation (y-axis) between input energy and AC (blue) vs. MC (green) as a function of constraint on input energy (x-axis) (mean and standard error over participants computed on Fisher transformed correlation coefficients are displayed). In case of low energy constraints, we observe a higher/lower correlation between input energy and MC/AC indicating that the optimal policy emphasizes high MC items. As energy constraints increase, this relationship is reversed, such that the policy favors allocating energy to high (as compared to low) AC nodes. (B) Squared error loss between the optimal state and the one-step ahead predicted observations depending on the optimal control policy identified for different values of ρ (x-axis) (mean over participants and standard error are displayed). The loss increases when energy constraints increase. Dashed lines indicate the mean trajectory loss and control energy empirically observed in the sample. (C) Identified treatment policies for a low (left) and high (right) constraint on input energy for one example participant and two selected variables. Calm* was the node with maximum AC, cheerful* the node with maximum MC for said participant. (D) Share of control energy in identified optimal policies on the highest AC/MC nodes for all participants (x-axes) for low energy constraints (left) vs. high energy constraints (right). (E) Control energy spent for low energy ($\rho = 0.1$; left) and high energy ($\rho = 100$; right) constraints on nodes sorted by high AC (blue) vs. MC (green) (mean over participants and standard error are displayed). (F) Predicted control policy for example participant for low energy ($\rho = 0.1$; left) and high energy ($\rho = 100$; right) constraints. The left panels display normalized AC and MC values (divided by the maximum value) for comparison purposes.

The inferred treatment policies were designed to improve the psychological state along all of its dimensions, driving all systems towards values of -3, delineating the most favorable mental health rating (cf. section Methods "Optimal control policies"). Figure 4a illustrates the relationship between exerted node-wise input energy and the previously described AC and MC metrics as a function of energy constraints. Figure 4b

depicts the exerted control energy for these constraints as well as the resulting deviation between desired and predicted trajectories, as well as empirically observed control energy and trajectory deviation for reference. Psychologically speaking, high energy constraints could for instance refer to situations in which we have limited possibilities of delivering an intervention, or to situations in which the delivered interventions have only limited effects (since in both of these situations, we can only exert a limited amount of control). In contrast, low energy constraints could refer to situations in which we can administer very effective interventions on a frequent basis. With only mild energy constraints, we observe a positive correlation between allocated input energy and MC, and a negative correlation with AC. In this case, the optimal control policy also allocates a higher total amount of control energy to the person-specific node with highest MC as compared to highest AC ($T(9) = -2.91, p = .017$, Figure 4c, d left). As energy constraints increase, this relationship is reversed, resulting in a high correlation between spent energy and AC (Figure 4a, blue line), and higher allocated energy on (person-specific) high AC nodes ($T(9) = 6.14, p < .001$; see Figure 4d right). As an example, Figure 4c depicts the allocated control energy of a recovered optimal control policy with low (Figure 4c left) and high (Figure 4c right) constraints on control energy. During low energy constraints, this policy would favor targeting feeling 'cheerful*' as compared to 'calm*', and vice versa for high energy constraints.

The increased emphasis on targeting high AC nodes in case of high energy constraints is consistent with the notion that when little energetic resources are available, more effective nodes need to be targeted to minimize the loss function (cf. eqn. (5)). In this case, the deviation between the reference trajectory (i.e., the state we want to drive the systems towards) and the trajectories predicted by the control policies will however increase (Figure 4b). This suggests that in the given sample, the high MC nodes are in fact superior in driving the system closer to the desired state (if we were free to control the system with arbitrary effort). For EMI based control policies, this would again indicate that in situations where we can flexibly target specific nodes, and have little restrictions on control, it may be favorable to target high MC over AC nodes (and vice versa). However, as Figure 4b also indicates, the mean empirically administered control energy is very low, suggesting that realistically, control input should be considered strongly constrained. Still, the optimal trajectory was closer on average to the target trajectory than the observed trajectories, showing that even in a setting with high costs of control, the potential to better allocate control energy (e.g., on high AC nodes in this case) exists.

Finally, we also asked whether optimal treatment policies were primarily driven by the perturbation of single or multiple nodes (i.e., targeting single or multiple psychological variables). The results are displayed in Figure 4e. As may be expected, during high energy constraints (Figure 4e right), the best intervention policy focuses on targeting a few high AC nodes, whereas during low energy constraints (Figure 4e left) the targets are more broadly distributed, with a slight preference for high MC nodes. This pattern is also reflected in individual optimal control sequences over time (see Figure 4f for an example for low (left) and high (right) control constraints).

3 Methods

3.1 Sample

The data analyzed here were collected as part of an uncontrolled pilot study that investigated the feasability, safety, and initial therapeutic effects of EMI - based on principles of compassion-focused therapy (CFT) - for enhancing resilience to stress in help-seeking youth. Please see Rauschenberg and colleagues [10] for elaborate details on study design, sample, inclusion and exclusion criteria, and data assessment. Briefly, the final sample consisted of ten individuals aged 14-25 years (mean 20.3 ± 3.8 years), with psychotic, depressive, or anxiety-related psychiatric symptoms and seeking help from secondary health services. The study was approved by the local ethics committee.

3.2 Empirical data

All study participants completed 3 weeks of EMI informed by EMA administered via a mobile app on a smartphone. During this period, participants were prompted 7 times per day on 6 consecutive days per week to complete a brief EMA. The EMA was scheduled at random times within predefined blocks of time. Whenever participants scored high on stress, negative affect and/or threat anticipation in the EMA (i.e., scores higher than 4 on a 7-point Likert scale), individuals were offered an EMI. The EMI consisted of four different exercises based on principles of CFT (for more information please see [10]). They served as real-time and real-world transfer of knowledge gained within three face-to-face sessions on CFT with a trained psychologist, supervised by an expert clinical psychologist in CFT, within a 3-week period (1 training session, 1 follow-up 'booster' session 2 weeks later, and 1 final review session).

3.2.1 EMA variables

For each EMA, participants were prompted to rate several scales related to positive and negative affect, social appraisals, physical needs, and more in their daily life. Table 1 summarizes the assessed EMA variables and associated statements which showed variation in all participants. EMA were assessed on a Likert scale (1 to 7, with 1=low, and 7=high) and were mean centered (-3 to 3) prior to analyses. Positive EMA variables (e.g., feeling 'cheerful') were inverted such that low values connote favorable health states in all cases. The inverted EMA are indexed by an asterisk (e.g., the inverted 'cheerful' scale is now denoted by 'cheerful*') to emphasize that low values indicate positive states (see Table 1).

3.2.2 EMA preprocessing

In order to infer the network structure and dynamics on these data, we first generated a data matrix $X = [x_0, x_1, ..., x_T]^\top \in \mathbb{R}^{(T+1)\times M}$ for each participant, in which the columns $x_{:,i}$ correspond to the $M = 15$ EMA items assessed at time points $t = 0, \ldots, T$ (listed in Table 1). A row of X, denoted by x_t, thus corresponds to a pattern of self-reports which we take to reflect a participant's (multivariate) mental health state at a given point in time. All EMA variables completed in response to one prompt were

treated as belonging to the same time point and thus allocated to the same bin (i.e., row of X). A bin was added whenever a prompt was answered. Missing values (which could occur if an EMA item was skipped or not prompted), were replaced by the last present value in the time series to avoid not-a-number values. Initial missing values (occurring before each item was fully prompted) were replaced by the grand average. Finally, only items which showed variation in each participant (that is, were not constant throughout the entire time series) were analyzed. For this proof-of-concept study, we intentionally refrained from other preprocessing steps (such as smoothing or other forms of imputation) to minimize assumptions made on the data.

3.2.3 EMI and input data

Details on the exact content of the presented compassion-focused EMI can be found elsewhere [10]. While the present analyses do not centrally focus on the content of these EMI, they were categorized into four qualitatively distinct types, referring to compassionate and positive imagery (EMI-I), compassionate self-validation (EMI-II), emotion as a wave (EMI-III), and compassionate writing (EMI-IV). Since not all participants completed EMI-IV, only the first three EMI entered our analyses. These three EMI were collected in binary column vectors $u_t \in \mathbb{R}^4$, with a non-zero element in the first, second, or third entry depending on which type was presented at a given time point. The fourth entry indicated whether a participant was currently alone (= 1) or in the presence of company (= 0) (termed 'with company'), as also assessed in the EMA. Given the relevance of social support and context for mental health [30], we therefore treated these four external inputs as inputs to the DS model (see next section).

3.3 Dynamical system models

To assess the network structure and its dynamics from these EMA and EMI time series (i.e., from x_t and u_t, $t = 0, \ldots, T$), we inferred (discrete time) linear dynamical systems (LDS) models of the form

$$x_{t+1} = Ax_t + Bu_t \tag{1}$$

where, once more, x_t corresponds to the $M = 15$ dimensional state (column) vector composed of EMA scores at time t (see Table 1), u_t corresponds to binary vectors coding for the 4 external inputs presented at time t, A is an adjacency matrix describing the interconnections and linear dynamics of states, and B is a regression coefficient matrix which maps the inputs onto the state variables. Each column of the regression coefficient matrix B thus corresponds to the inferred perturbation of the respective input. This model corresponds to an order 1 vector autoregressive model (VAR) (with 0 bias and no noise) where A and B were inferred via regularized least squares using ridge regression. The regularization strength of the ridge regression was determined per model and set to the minimum value at which the inferred system was stable (that is, the maximum absolute eigenvalue of A was smaller than 1), and varied between 0 and 1.5 (see also [22, 31] for discussions on modeling affect dynamics with VAR models).

To assess the agreement between true and model predicted data, we assessed the explained variation R^2 for each EMA time series (by computing the average squared correlation coefficient between true and predicted time series across participants). To assess the agreement between true and predicted immediate input effects, we compared the difference between true EMA scores immediately before and after an external input to the difference between EMA scores immediately before and *predicted* EMA scores immediately after an input.

3.4 Controllability and DS analysis

Eqn. 1 defines a map that describes the temporal evolution of the vector-valued mental health state. Through matrix A, the nodes $x_{:,i}$ (i.e., the EMA variables) form an interconnected network. Here, using NCT, we aim to quantify how the different nodes, and input to these nodes, control the temporal evolution of the inferred systems (i.e., the network dynamics), and how this control is constrained by the inferred network structure. We briefly mention that network controllability is mathematically studied by representing the network in terms of a graph $\mathcal{G} = (\mathcal{V}, \mathcal{E})$, where $\mathcal{V}$ are the vertices (or nodes), and $\mathcal{E}$ are edges of the graph (see also Figure 2c). Here, matrix $A = [a_{ij}]$ relates to the weighted adjacency matrix of $\mathcal{G}$, where a_{ij} quantifies the edges between pairs of vertices, and the real-valued EMA variables are associated with the graph's vertices.

In NCT, the controllability Gramian is a matrix that contains information on the ability and the degree to which an external input exerts control over a DS. To understand this matrix more intuitively, we first define the (T-step) controllability matrix as

$$C_T = \left[\tilde{B}\ A\tilde{B}\ A^2\tilde{B}\ \cdots\ A^{T-1}\tilde{B}\right].$$

Here, $\tilde{B}$ corresponds to a matrix or vector, in the following referred to as 'control vector', which specifies the nodes which are targeted and the degree to which they are targeted by an external input (also referred to as 'control input'). For instance, $\tilde{B}$ could correspond to columns of B (cf. eqn. (1)), if we were to test the controllability of the presented EMI. It could however, more generally refer to any other perturbation a participant was exposed to, or not exposed to, in the case that we want to evaluate effects of simulated hypothetical perturbations. The elements of C_T correspond to the system's response to a control vector and single control input of 1 (collectively referred to as intervention in the following) at consecutive moments in time, also referred to as the system's cumulative impulse response [26]. As an example, they could correspond to iterations of the map in eqn. (1) starting from an initial state $x_0 = 0$ and control vector $B_{:,i}$ presented at $t = 0$. The (T-step) controllability Gramian is directly associated with the controllability matrix, given by

$$W_T \coloneqq C_T C_T^\top = \sum_{t=0}^{T-1} A^t \tilde{B}\tilde{B}^\top (A^\top)^t. \tag{2}$$

Eigenvectors and eigenvalues of W_T correspond to directions in state space and the relative ease to steer system into them. Eigenvectors associated to large (small) eigenvalues correspond to easily (difficult) to control directions, that is, it requires a low/high amount of input energy [26, 29]. Many controllability metrics are therefore defined in terms of the eigenvalues of this Gramian.

3.4.1 Controllability

We first assessed whether the inferred systems were generally controllable by the presented EMI or by simulated interventions on single network nodes. A system is controllable in T time steps by a control vector, if for any initial state x_0 and final state x_T of the system, there exists a control input sequence $u_0, \ldots, u_{T-1}$, that steers the system from x_0 to x_T [32]. In other words, the EMA networks are structured in a way that we could, in theory, leverage the proposed interventions to drive the system into any state we aim for. For a system to be controllable in T time steps, W_T has to have all non-zero eigenvalues (since an eigenvalue of 0 indicates directions the system cannot move in), which implicates that W_T has full rank. For a system to be controllable, it needs to be controllable in $T = M$ time steps (M being the size of the system; [26]). Controllability was therefore assessed by checking the rank of W_T, with $T = M$, for the case where $\tilde{B}$ was set either to columns of B (eqn. (1)), or to unit (canonical) vectors targeting each node separately (multiplied by -1 to account for positive effects on mental health).

3.4.2 Average controllability

AC determines interventions on a network that may drive a system into different states with little (input) energy [27]. In other words, AC quantifies the relative efficiency of an intervention. We quantify AC here as AC = trace(W_T), with $T = M$ as above [29, 33]. To assess the AC of the actual presented inputs (including the EMI), we set $\tilde{B}$ to the inferred input effects, that is, to columns of B (cf. eqn. (1)). To assess the AC of simluated hypothetical interventions targeted at single network nodes, we set $\tilde{B}$ to negative unit vectors $-e_j$.

3.4.3 Modal controllability

Since AC is strongly dominated by the largest eigenvalues of W_T which indicate easily reachable directions given an intervention, AC rather measures the ability of a node to steer the system into easily controllable directions with little input energy. In contrast, MC identifies network nodes that can, in principle, also steer the system towards hard-to-reach configurations. MC does not depend on input but is a property of the network, where the MC of node i is given by

$$\mathrm{MC}_i = \sum_{j=1}^{M} \left(1 - |\lambda_j|^2\right) |\nu_{ij}|^2. \tag{3}$$

Here, j refers to the j-th eigenvalue of the participant specific adjacency matrix A, and ν_{ij} is the i-th component of the j-th eigenvector of A. Loosely speaking, since

ν_{ij} denotes the projection of x_i onto the j-th eigenvector or mode (i.e., independent direction a system may move in), and j the degree of change in eigenvector direction, MC quantifies the controllability or reach of node i on all of its modes. A high reach may imply that a node is able to steer the state into directions difficult to reach with low input energy.

3.4.4 Cumulative impulse response

The metrics introduced so far conveniently assign single numbers relating to different aspects of controllability. Sometimes we may be more interested in quantifying the behavior of the system in terms of the actual observed measurements. As indicated earlier, the system's CIR quantifies the future output of a system in response to an initial input. To assess the predicted effects of targeting single network nodes, as well as targeting multiple nodes by the presented inputs, on the actual EMA item scores, we computed the associated effects vectors

$$\mathrm{CIR}_T = \sum_{t=0}^{T} A^i \tilde{B} \tag{4}$$

where the $j-$th component of CIR_T represents the total effect on observable j of the intervention defined by control vector $\tilde{B}$ after applying a control input once at time $t = 0$, and accumulating effects over time (see also [17]). Once more, we set $\tilde{B}$ to columns of B to compute CIRs for the presented inputs, and to negative unit vectors $-e_j$ to compute CIRs for simulated interventions which target single network nodes. The minus sign accounts for simulating interventions with positive effects on mental health. T was set to 100 to account for a sufficient temporal horizon. To compare CIRs between different inputs, dependent samples t-tests were applied and Bonferroni corrected for multiple comparisons where appropriate.

3.4.5 Optimal control policies

Beyond control metrics, NCT provides principled approaches towards obtaining optimal control sequences. The optimal control sequence $U^* = u_0^*, \ldots, u_{T-1}^*$ refers to the unique sequence of inputs which will drive a given system towards a desired state while minimizing some loss function. Without specifying the loss, there are (infinitely) many such sequences. However, some of these sequences could require an intense amount of input energy whereas others could take an exceedingly high amount of time. The loss function thus typically regulates how fast we want the system to converge to the desired state, and how much input energy we want to provide along the way (or in other words, how costly we define our inputs to be). If the loss function is convex, this optimization problem under constraints is well defined [26]. The most commonly used loss function in this context is

$$L = x_T^\top Q x_T + \sum_{t=0}^{T-1} (x_t^\top Q x_t + u_t^\top R u_t)$$

where Q and R are self-determined matrices which penalize the speed of convergence and the enforced input energy, respectively. For instance, if we consider inputs to be very costly and therefore aim at identifying a control sequence with little input energy, we can increase the values in R. Alternatively, if we increase Q, we emphasize that we want fast convergence to our desired state. The algorithm that minimizes the above loss for a model as in eqn. (1) is commonly known as the Linear Quadratic Regulator (LQR). It will identify a policy that stabilizes the system, i.e., aims at driving the system towards 0 (its fixed point). In our experimental case, however, the most desirable state is reached at values of -3. To account for this offset, we define a reference trajectory $r_0, \ldots, r_T$, rewriting the loss as

$$L = (x_T - r_T)^\top Q(x_T - r_T) + \sum_{t=0}^{T-1} \left((x_t - r_t)^\top Q(x_t - r_t) + u_t^\top R u_t \right). \tag{5}$$

This will encourage a control input solution that drives the system towards the defined reference trajectory. The reference trajectory in principle allows for user-defined outcome goals (e.g., by setting only specific values in the reference trajectory to -3). For the system given in eqn. (1) and the loss given in eqn. (5), we can analytically obtain the optimal control input sequence U^* such that L is minimized. At any given time point, the optimal control depends only on the current state of the trajectory, but not its past or future, resulting in the possibility to update the policy online while data collection is ongoing.

We first computed the optimal control solutions fixing Q (i.e. convergence speed) to the identity and varying the penalization of control input $R = \rho I$ by $\rho \in [0.1, 100]$. As ρ increases, we are therefore simulating scenarios in which we can only expect very limited effects, or more precisely, may only exert little control over our state with the presented treatments. We then related the exerted (node-wise) control energy $E_i = \sum_{t=0}^{T-1} (u_t)_i^2$ of the respective recovered control sequence to AC and MC measures (for more elaborate details on how the optimal control input sequence was obtained please see Supplement "Methods").

4 Discussion

The delivery of EMI within the naturalistic daily life setting of an individual bears great potential for mental health promotion, prevention, and treatment of mental health conditions [7, 9]. The assessment of psychological variables relating to overall mental health using EMA allows for a detailed and ecologically valid measurement of proximal outcomes of EMI. However, accurate evaluation of proximal intervention effects, mechanisms of change, and intervention placement presents novel challenges due to the temporal dynamics of underlying psychological states and their interactions [16, 17, 34]. To address these challenges, we propose a control theoretic approach that has, to the best of our knowledge, not yet been applied to EMA and EMI. The approach considers EMA variables as part of a network of interconnected states [15, 17, 21, 35], whereas interventions constitute perturbations to these states. NCT facilitates the study and evaluation of network perturbations at the level of an individual. It may also

help us design and predict effects of (novel) personalized treatment delivery schemes based on a principled approach. Here, we demonstrate how perturbation analyses can be deployed to better understand and systematically study EMA networks. In particular, we use NCT to evaluate real and simulated intervention effects, to thereby gain insight into network mechanisms, and to guide delivery schemes under considerations of energetic and temporal constraints.

Current findings

We inferred linear dynamical systems models from the EMA time series of each participant and examined the impact of real and simulated inputs using concepts from NCT. This led to several important insights. The predicted proximal effects of the investigated external inputs as well as simulated inputs were largely consistent with prior expectations. For instance, simulated interventions which perturbed the systems into a positive mental health direction (e.g., by reducing social unpleasantness' or increasing cheerfulness) exerted an overall positive effect on mental health. Moreover, the administered EMI also resulted in an overall pattern of improvement across predicted psychological variables, and exerted a stronger degree of system control than the mere (passive) indication of social presence and absence. This aligns well with previous observations of immediate EMI-driven mental health improvements [10], as well as the general motivation behind delivering these specific EMI (e.g., [11, 36]). The consistency of these findings w.r.t. expectations speaks to the validity of the proposed approach.

Although expected and predicted mental state changes aligned well, we also found large inter-individual differences in dynamical systems and system responses, that is, both in terms of network connections as well as in AC and CIR. This variability implicates that interventions are likely to affect each individual differently and indicates the necessity to harmonize an individual's personal dynamics with the proposed interventions (see also [19, 20]). Consistent with this idea, we found that a personalized (simulated) intervention targeted at the participant-specific node with highest AC predicted a larger improvement in mental health state than a group-based intervention strategy. AC (perhaps combined with CIR) could thus be a good indicator for a personalized delivery scheme.

Finally, using the linear quadratic regulator, we assessed optimal intervention delivery schemes (referred to as "optimal control policies"), to gain additional insights into suitable strategies for mental health promotion, prevention, and treatment of mental health conditions. For each participant, we determined this optimal delivery scheme as a function of energy constraints. This may roughly be understood as how the sequence of proposed optimal interventions changes, depending on whether we can afford to strongly and frequently perturb the system of a given participant, or not. Limits on the beneficial effects or possible frequency of a proposed intervention may thus be seen as an energy constraint. In the context of the psychological networks examined here, we observed that energy constraints modulate whether the intervention strategy should focus on targeting nodes with high modal vs. high average controllability. When energy resources are freely available (i.e., we can deliver interventions frequently and may expect a strong impact), then more emphasis (i.e., control energy) should be allocated

to nodes with high MC. If this is not the case, then the intervention strategy shifts ever more to focus on (few) nodes with high AC. The stronger and narrower allocation of energy on high AC nodes during high energetic constraints is intuitive. Under these circumstances, intervention strategies should progressively focus on interventions that drive large (positive) changes with little effort. Interestingly, these observations were driven by group analyses suggesting that whereas MC and AC may substantially vary across individuals, the optimal delivery scheme follows similar energetic trade-off principles. Considerations on energetic constraints may thus play a substantial role for the design of an optimal intervention delivery scheme.

Implications for EMI delivery schemes and evaluation

Based on these findings, we see several promising future directions for NCT and EMI research. First off, while intuitive, energetic considerations are not commonly factored in when designing intervention strategies. Integrating psychotherapeutic research that focuses on designing interventions specifically targeted at changing an individual's mental state "in the moment" with aspects of dynamical systems and control could prove particularly profitable to improve future EMI delivery schemes. As an example, the EMI selected in the current data set are based on principles of CFT that rest on cultivating and enhancing compassion in individuals. These compassion focused interventions (CFIs) are particularly designed to act on three interacting emotional systems - the soothing, the drive, and the threat system - and use intervention techniques (e.g., positive mental imagery) expected to exert momentary (i.e., "in-the-moment") effects on mental health [36]. For instance, by strengthening the soothing system, CFIs may down-regulate the threat-system and up-regulate the drive system, resulting in an overall mental health improvement. By capturing the dynamics of these emotional systems and integrating a preselected set of EMI targeted at these systems into a delivery scheme that selects a personalized EMI based on the proximal prediction of its effects under considerations of energetic constraints, we can hope to place and exploit these interventions more optimally.

As an example, one such strategy could rest on leveraging dynamical system models to forecast EMI effects (e.g., by assessing their CIR) and probabilistically selecting the most promising one (see e.g., https://ai4u-training.de/). Alternatively, to account for strong energetic constraints, the selection algorithm could additionally factor in AC (e.g., by probabilistically selecting the EMI with largest AC, or by linking AC and CIR). Our simulated analyses demonstrate that this could in fact be an effective approach. Ideally though, in analogy to the linear quadratic regulator, we would have an algorithm which renders an optimal delivery scheme based on a set of predefined binary inputs and control matrix (as is the case with the EMI, cf. section 3.2.3), as well as possible temporal constraints on delivery time points (to account for the circumstance that we cannot present an EMI at each moment). So far, optimal control sequences in NCT are conventionally identified under the premise that interventions can be scaled (as for instance in the case of a car which is controlled by the precise dosage and addition of fuel). The development of optimal control algorithms that address the specific requirements of EMI may be extremely powerful in this context.

Moreover, in combination with real-time model inference and closed-loop control laws [26], such algorithms could be successively adapted and optimized [34, 37]. Iterative inference and control approaches could also circumvent or counteract issues which arise due to nonstationarities, i.e., when the observed statistical distributions associated with an individual's response pattern (and associated underlying generative network) changes over time [38]. In an iterative inference protocol, models could be inferred on a fixed number of past responses, thus neglecting distant data with other distributional properties. Alternatively, such protocols could first detect nonstationarities and then base model inference on identified stationary chunks of the data.

Beyond informing EMI delivery schemes, assessing network control metrics may prove valuable more generally when evaluating and interpreting intervention effects. For instance, assessing whether a psychological network is at all controllable by a specific intervention can provide a quick marker of whether certain state configurations are at all reachable, and could further be complimented by analyses unmasking which dimensions are unreachable (e.g., by looking at minimal controllability; [29]).

Network CIRs and ACs are simple and interpretable quantities that capture proximal intervention effects and can help us gain insight into behavioral contingencies and network mechanisms [27, 39]. This is important since interactions between network nodes are often not immediately evident from inspecting observed time series, or may even entirely elude our observation [17, 24]. Moreover, we can leverage this approach to study both the effects of actual EMI, as well as effects of simulated interventions targeted at specific network nodes. The latter can be exploited to gain additional insights into yet unexplored network mechanisms and behavioral contingencies [27, 39]. Such analyses may prove invaluable to provide personalized feedback to users and increase awareness w.r.t. an individual's personal behavioral contingencies. For instance, one could inform on interactions between psychological variables (e.g., 'when you are not relaxed, you tend to feel less appreciated'), educate on the effects of a given CFI (e.g., 'positive imagery relaxes you'), and raise awareness for effects of other recorded external factors (e.g., 'spending time in nature had a positive effect on your mood'). In blended care settings, such evaluations could even inform the therapist on possible effective leveraging points.

Limitations

The success of the proposed approaches will likely rest on the ability of the DS model to reconstruct the correct (or close to correct) dynamics (as also pointed out in [17]; see also [40]). While they may not be an adequate reflection of reality, linear models have proven to be good approximations to many systems [41], and are frequently deployed in this or similar contexts [22, 42]. Also, linear models of equal dimension to the observable space may better account for the bias-variance trade-off in the context of these comparatively short time series [43, 44]. Nonetheless, more powerful nonlinear approaches to reconstruct dynamics from time series exist (as reviewed in [40]; see also [45, 46]). On the downside, given their complexity, these approaches likely require longer time series to generalize well, and NCT is more easily applied to linear systems.

Optimal control algorithms with input constrained to finite EMI sets have yet to be developed for complex nonlinear models.

Future studies should concentrate on validating the proposed approaches on longer time series. By inferring models on part of the time series and predicting the statistics of the left-out part, we could validate the here-made observations on a personalized level [44, 47]. For instance, an out-of-sample prediction error could quantify the deviation of predicted CIR and actual CIR, or the inferred dynamics more generally, as well as evaluate the proposed intervention delivery schemes.

Concluding remarks

The proposed approach complements and extends proposed network theories of mental disorders [15, 48]. The general view here is that mental disorders arise through the coordinated interaction between a network of mental health symptoms [15], or underlying latent variables [38]. Internal or external factors which influence single symptoms will therefore also change other causally connected symptoms. This perspective rather seamlessly accounts for frequently observed phenomena including the self-sustaining negative effect of a momentary adverse experience on mental health, as well as explanations for vulnerability and resilience mechanisms [15]. Methods that shed light onto network interaction and feedback mechanisms will therefore putatively help to improve our understanding on the etiology of mental disorders. NCT may be understood as one such framework that directly quantifies the degree of control network nodes exert over each other and accounts for essential dimensions such as energetic and temporal constraints. This augments more traditional network analysis approaches that study network centrality indices [49], as well as recent advanced approaches to study node importance in psychological networks [50]. Considering node importance through the lens of network control directly relates network dynamics to intervention policies. The same NCT framework as adopted in the present study may be easily transferred to latent variable models (in which case eqn. (1) is simply coupled to an additional observation model [26]), and may also reflect a very powerful approach to study EMA dynamics [38].

Administering effective personalized mHealth interventions and discovering the mechanisms underlying interindividual differences in intervention response are two central goals in current digital mental health research. EMA provide exceptional opportunities to study effects of EMI as well as simulated interventions on mental health, by assessing relevant psychological variables and their temporal evolution over long time windows. By understanding these variables as part of a DS that responds to perturbations, NCT comprises a natural way of addressing both goals of digital mental health research. Personalized intervention effects correspond to the control these interventions exert over a specific system. Perturbation analyses, hypothetical or real, provide insights into contingencies between psychological variables and thus elucidate behavioral contingencies and action mechanisms. Network control algorithms reveal important insights into personalized optimal delivery schemes.

Acknowledgments

This work was funded by a living lab grant by the Federal Ministry of Science, Education and Culture (MWK) of the state of Baden-Wurttemberg, Germany (grant number 31-7547.223-7/3/2) and the European Union's Horizon 2020 research and innovation programme under grant agreement 945263 (IMMERSE) to DD, GK, and UR, by the German Research Foundation (DFG) within the collaborative research center TRR-265 (project A06) to DD and GK, and by a DFG Heisenberg professorship (No. 389624707) to UR. The funder played no role in study design, data collection, analysis and interpretation of data, or the writing of this manuscript.

Declarations

Author contributions

JF and GK conceptualized the work, performed the analyses, and drafted the first version of the manuscript. CR, BB, TVA, UR were involved in data collection through conceptualizing, designing, conducting, and/or acquiring funds for the original pilot study. These authors all contributed to writing, reviewing, and editing the pilot study in which the data was collected. CR, HJ, DD, and UR thoroughly reviewed and revised the manuscript, contributing novel ideas and interpretations of the data. All authors edited and approved the manuscript draft.

Conflicts of interest

Authors JF, CR, HJ, BB, TVA, UR, DD, GK declare no financial or non-financial competing interests.

Data and code availability

All code used for data analysis and figure generation have been made publicly available at JF's personal Github page. Data will be made available upon reasonable request to the authors.

Tables

Appendix A Optimal control policies

In the following, we state the solution to obtain an optimal control policy based on the specified loss function (eqn. (5), main manuscript), and refer the reader to [32] for a more comprehensive understanding of the involved derivations. Optimizing the loss function yields the following solution to obtain the optimal control input:

$$u_t = -G_t x_t + F_t v_{t+1}.$$

Table 1 EMA variables across participants. Inverted variables are highlighted by an asterisk.

EMA label	EMA statement
Act. unpleasant	I find [this activity] unpleasant
Agreeable*	I find this pleasant
Soc. apprec.*	I feel appreciated
Soc. unpleasant	I find this company unpleasant
Rather company	I would prefer to be in the company of other people
Choose alone*	I choose to be alone [when alone]
Hungry	I feel hungry
Energetic*	I feel energetic
Calm*	I feel calm
Uncomfortable	I feel uncomfortable
Relaxed*	I feel relaxed
Irritated	I feel irritated
Down	I feel down
Cheerful*	I feel cheerful
Anxious	I feel anxious

The so-called feedback term, $G_t x_t$, contains information from the current trajectory. G_t is the (Kalman) gain matrix given by

$$G_t = \left(B^\top S_t B + R\right)^{-1} B^\top S_t A,$$

where S_t is obtained by the recursive Riccati equation

$$S_t = A^\top S_{t+1} \left(A - B \left(B^\top S_{t+1} B + R\right)^{-1} B^\top S_{t+1} A\right) + Q,$$
$$S_T = Q.$$

Q and R have been defined along with the loss function and must be positive semidefinite (R positive definite). The so-called feedforward term $F_t v_{t+1}$ contains information from the future steps of the reference trajectory. It is transmitted via the adjoint state v_{t+1}, recursively given by

$$v_t = \left(A - BG_t\right)^\top v_{t+1} + Q r_t,$$
$$v_T = Q r_T.$$

Finally, F_t is another gain matrix given by

$$F_t = \left(B^\top S_t B + R\right)^{-1} B^\top.$$

Since it usually converges quickly, S_t can be replaced by its limit, the solution of the Algebraic Riccati equation

$$S = A^\top \left(S - SB \left(B^\top SB + R\right)^{-1} B^\top S\right) A + Q,$$

to save memory cost. This results in constant gain matrices F and G. Because the exact solution to v_t depends on a time-varying gain, an approximation can be obtained

by iterating through to v_0 and then setting

$$v_{t+1} = (A - BG)^\top v_t - \left((A - BG)^\top\right)^{-1} Q r_t.$$

References

[1] Myin-Germeys, I. *et al.* Experience sampling research in psychopathology: opening the black box of daily life. *Psychological Medicine* **39**, 1533–1547 (2009).

[2] Schick, A. *et al.* Effects of a novel, transdiagnostic, hybrid ecological momentary intervention for improving resilience in youth (EMIcompass): protocol for an exploratory randomized controlled trial. *JMIR Research Protocols* **10**, e27462 (2021).

[3] Shiffman, S., Stone, A. A. & Hufford, M. R. Ecological momentary assessment. *Annual Review of Clinical Psychology* **4**, 1–32 (2008).

[4] Trull, T. J. & Ebner-Priemer, U. W. Using experience sampling methods/ecological momentary assessment (ESM/EMA) in clinical assessment and clinical research: introduction to the special section [editorial]. *Psychological Assessment* **21**, 457–462 (2009).

[5] Myin-Germeys, I. *et al.* Experience sampling methodology in mental health research: new insights and technical developments. *World Psychiatry* **17**, 123–132 (2018).

[6] Reichert, M. *et al.* Ambulatory assessment for precision psychiatry: Foundations, current developments and future avenues. *Experimental Neurology* **345**, 113807 (2021).

[7] Schulte-Strathaus, J. C., Rauschenberg, C., Baumeister, H. & Reininghaus, U. in *Ecological momentary interventions in public mental health provision* 427–439 (Springer, 2022).

[8] Heron, K. E. & Smyth, J. M. Ecological momentary interventions: incorporating mobile technology into psychosocial and health behaviour treatments. *British Journal of Health Psychology* **15**, 1–39 (2010).

[9] Myin-Germeys, I., Klippel, A., Steinhart, H. & Reininghaus, U. Ecological momentary interventions in psychiatry. *Current Opinion in Psychiatry* **29**, 258–263 (2016).

[10] Rauschenberg, C. *et al.* A compassion-focused ecological momentary intervention for enhancing resilience in help-seeking youth: uncontrolled pilot study. *JMIR Mental Health* **8**, e25650 (2021).

[11] Reininghaus, U. *et al.* Effects of a novel, transdiagnostic ecological momentary intervention for prevention, and early intervention of severe mental disorder in youth (emicompass): Findings from an exploratory randomized controlled trial. *Schizophrenia Bulletin* **49**, 592–604 (2023).

[12] Schueller, S. M., Aguilera, A. & Mohr, D. C. Ecological momentary interventions for depression and anxiety. *Depression and Anxiety* **34**, 540–545 (2017).

[13] Bell, I. H., Lim, M. H., Rossell, S. L. & Thomas, N. Ecological momentary assessment and intervention in the treatment of psychotic disorders: a systematic review. *Psychiatric Services* **68**, 1172–1181 (2017).

[14] McDevitt-Murphy, M. E., Luciano, M. T. & Zakarian, R. J. Use of ecological momentary assessment and intervention in treatment with adults. *Focus* **16**, 370–375 (2018).

[15] Borsboom, D. A network theory of mental disorders. *World Psychiatry* **16**, 5–13 (2017).

[16] Boruvka, A., Almirall, D., Witkiewitz, K. & Murphy, S. A. Assessing time-varying causal effect moderation in mobile health. *Journal of the American Statistical Association* **113**, 1112–1121 (2018).

[17] Henry, T. R., Robinaugh, D. J. & Fried, E. I. On the control of psychological networks. *Psychometrika* **87**, 188–213 (2022).

[18] Rabbi, M., Klasnja, P., Choudhury, T., Tewari, A. & Murphy, S. Optimizing mHealth interventions with a bandit. *Digital Phenotyping and Mobile Sensing: New Developments in Psychoinformatics* 277–291 (2019).

[19] Bidargaddi, N., Schrader, G., Klasnja, P., Licinio, J. & Murphy, S. Designing m-Health interventions for precision mental health support. *Translational Psychiatry* **10**, 222 (2020).

[20] Nahum-Shani, I. *et al.* Just-in-time adaptive interventions (JITAIs) in mobile health: key components and design principles for ongoing health behavior support. *Annals of Behavioral Medicine* **52**, 446–462 (2018).

[21] Bringmann, L. F. *et al.* Psychopathological networks: Theory, methods and practice. *Behaviour Research and Therapy* **149**, 104011 (2022).

[22] Hamaker, E. L., Ceulemans, E., Grasman, R. & Tuerlinckx, F. Modeling affect dynamics: State of the art and future challenges. *Emotion Review* **7**, 316–322 (2015).

[23] Hofmann, S. G., Curtiss, J. & McNally, R. J. A complex network perspective on clinical science. *Perspectives on Psychological Science* **11**, 597–605 (2016).

[24] Stocker, J. E. *et al.* Towards a formal model of psychological intervention: Applying a dynamic network and control approach to attitude modification. *PsyArXiv* (2022).

[25] Wigman, J. T. *et al.* Psychiatric diagnosis revisited: towards a system of staging and profiling combining nomothetic and idiographic parameters of momentary mental states. *PLoS One* **8**, e59559 (2013).

[26] Brunton, S. L. & Kutz, J. N. *Data-driven science and engineering: Machine learning, dynamical systems, and control* (Cambridge University Press, 2022).

[27] Gu, S. *et al.* Controllability of structural brain networks. *Nature Communications* **6**, 1–10 (2015).

[28] Karrer, T. M. *et al.* A practical guide to methodological considerations in the controllability of structural brain networks. *Journal of Neural Engineering* **17**, 026031 (2020).

[29] Pasqualetti, F., Zampieri, S. & Bullo, F. Controllability metrics, limitations and algorithms for complex networks. *IEEE Transactions on Control of Network Systems* **1**, 40–52 (2014).

[30] Turner, R. J. & Brown, R. L. Social support and mental health. *A handbook for the study of mental health: Social contexts, theories, and systems* **2**, 200–212 (2010).

[31] Jordan, D. G., Winer, E. S. & Salem, T. The current status of temporal network analysis for clinical science: Considerations as the paradigm shifts? *Journal of clinical psychology* **76**, 1591–1612 (2020).

[32] Lewis, F. L., Vrabie, D. & Syrmos, V. L. *Optimal control* (John Wiley & Sons, 2012).

[33] Summers, T. H., Cortesi, F. L. & Lygeros, J. On submodularity and controllability in complex dynamical networks. *IEEE Transactions on Control of Network Systems* **3**, 91–101 (2015).

[34] Koppe, G., Guloksuz, S., Reininghaus, U. & Durstewitz, D. Recurrent neural networks in mobile sampling and intervention. *Schizophrenia Bulletin* **45**, 272–276 (2019).

[35] Bringmann, L. F., Lemmens, L. H., Huibers, M. J., Borsboom, D. & Tuerlinckx, F. Revealing the dynamic network structure of the Beck Depression Inventory-II. *Psychological Medicine* **45**, 747–757 (2015).

[36] Paetzold, I. *et al.* A hybrid ecological momentary compassion–focused intervention for enhancing resilience in help-seeking young people: Prospective study of

baseline characteristics in the emicompass trial. *JMIR Formative Research* **6**, e39511 (2022).

[37] Durstewitz, D., Koppe, G. & Meyer-Lindenberg, A. Deep neural networks in psychiatry. *Molecular Psychiatry* **24**, 1583–1598 (2019). Number: 11.

[38] Bringmann, L. F., Ferrer, E., Hamaker, E. L., Borsboom, D. & Tuerlinckx, F. Modeling nonstationary emotion dynamics in dyads using a time-varying vector-autoregressive model. *Multivariate Behavioral Research* **53**, 293–314 (2018).

[39] Lynn, C. W. & Bassett, D. S. The physics of brain network structure, function and control. *Nature Reviews Physics* **1**, 318–332 (2019).

[40] Durstewitz, D., Koppe, G. & Thurm, M. I. Reconstructing Computational Dynamics from Neural Measurements with Recurrent Neural Networks. *bioRxiv* (2022).

[41] Kirk, D. E. *Optimal control theory: an introduction* (Courier Corporation, 2004).

[42] Peralta, V., Gil-Berrozpe, G. J., Librero, J., Sánchez-Torres, A. & Cuesta, M. J. The symptom and domain structure of psychotic disorders: a network analysis approach. *Schizophrenia Bulletin Open* **1**, sgaa008 (2020).

[43] Hastie, T., Tibshirani, R., Friedman, J. H. & Friedman, J. H. *The elements of statistical learning: data mining, inference, and prediction* Vol. 2 (Springer, 2009).

[44] Koppe, G., Meyer-Lindenberg, A. & Durstewitz, D. Deep learning for small and big data in psychiatry. *Neuropsychopharmacology* **46**, 176–190 (2021).

[45] Brenner, M., Koppe, G. & Durstewitz, D. Multimodal Teacher Forcing for Reconstructing Nonlinear Dynamical Systems. *arXiv* (2022).

[46] Kramer, D., Bommer, P., Tombolini, C., Koppe, G. & Durstewitz, D. Reconstructing Nonlinear Dynamical Systems from Multi-Modal Time Series. *Proceedings of the 39th International Conference on Machine Learning (PLMR)* **162**, 1–21 (2022).

[47] Thome, J. *et al.* Model-based experimental manipulation of probabilistic behavior in interpretable behavioral latent variable models. *Frontiers in Neuroscience* **16**, 2270 (2023).

[48] Fried, E. I. & Cramer, A. O. Moving forward: Challenges and directions for psychopathological network theory and methodology. *Perspectives on Psychological Science* **12**, 999–1020 (2017).

[49] Borsboom, D. & Cramer, A. O. Network analysis: an integrative approach to the structure of psychopathology. *Annual Review of Clinical Psychology* **9**, 91–121 (2013).

[50] Bringmann, L. F. *et al.* What do centrality measures measure in psychological networks? *Journal of Abnormal Psychology* **128**, 892–903 (2019).